

## RELIABILITY-BASED CALIBRATION OF PARTIAL FACTOR FOR THIN NON-STRUCTURAL ELEMENTS MADE OF UHPFRC

Svatopluk Dobrusky (1), Sébastien Bernardi (2) and Seddik Sakji (3)

(1) LafargeHolcim Research Centre, France

(2) Ductal®, France

(3) Centre Scientifique et Technique du Batiment, France

### Abstract

Current design codes are based on a semi-probabilistic approach which requires calibrated partial factors to secure the safety of structures and people. The current code calibration procedures do not reflect the development of computation tools and improved knowledge of structural design. Moreover, the current procedure neglects economic aspects which should be an integral part of any code calibration. This article presents a modified approach of the reliability-based code calibration applied to UHPFRC thin elements predominantly loaded in bending. The modified approach eliminates disadvantages of the original procedure and it is defined in a way to take advantage of the current computation means such as parallel and cloud computing. Moreover, the removal of the iterative loop allows using Monte Carlo methods (among other options) which are normally time-consuming and impractical for code calibration. The new design verification of UHPFRC with the newly calibrated partial factors allows better exploitation of the material without compromising the safety requirements.

### Résumé

Les codes de conception actuels sont basés sur une approche semi-probabiliste qui nécessite des coefficients partiels calibrés pour assurer la sécurité des structures et des personnes. Les procédures actuelles de calibrage de code ne reflètent pas le développement des outils de calcul informatique et l'amélioration des connaissances en matière de conception structurelle. En outre, la procédure actuelle néglige les aspects économiques qui devraient être partie intégrante de tout code de calibrage. Cet article présente une approche modifiée du calibrage fiabiliste du code appliquée aux éléments minces en BFUP principalement chargés en flexion. L'approche modifiée élimine les inconvénients de la procédure d'origine et est définie de façon à tirer profit des moyens de calcul actuels, tels que le calcul parallèle et en réseau. De plus, l'élimination des boucles d'itération permet d'utiliser les méthodes Monte-Carlo (entre autres) qui sont habituellement très coûteuses en temps et peu pratiques pour la calibration des codes. Les nouvelles règles de justification des structures en BFUP avec les coefficients partiels nouvellement calibrés permettent de mieux tirer parti du matériau sans compromettre les exigences de sécurité.

## 1. INTRODUCTION

Although many applications of UHPFRC have been constructed, there is still a limited amount of design norms for such a material which can be used. The lack of design norms is probably the biggest obstacle for broader applications of the material with such a potential. Fortunately, the recent French and Swiss norms represent a great step forward for UHPFRC users and producers.

Nevertheless, despite the fact that these documents are very useful, none of them sufficiently covers the domain of the architectural non-structural applications. AFGC 2013 [1] describes a simplified constitutive law for thin elements (chapter 2), three back analyses methods for determining the constitutive law (annex 4), and a few recommendations on general aspects. Unfortunately, the disunited paragraphs have made the design of thin elements according to the recommendations an impractical option. As the result, product certifications in France for thin elements made of UHPFRC have been evaluated and certified according to a brittle-failure-like design. The brittle-failure approach is based on an elastic response of the material with the global safety factor of 3. However, the brittle failure is avoided by the fibers in the matrix. Moreover in many cases, the fibers improve Modules of Rapture (MOR) which can be significantly higher than Limit of Proportionality (LOP). The long-standing experience of facade panel designs made of UHPFRC proves that the current approach, based on the global safety factor for LOP, is too restrictive as it does not take into account any contribution of the fibers.

Hence, C.S.T.B. (“Centre Scientifique et Technique du Batiment”, French regulatory organization) decided to set a working group involving precasters and contractors with an objective to introduce a semi-probabilistic design method, for the thin UHPFRC elements, which would be coherent with Eurocodes [2, 3, 4, 5], French UHPFRC standards and AFGC 2013 [1] recommendations. The new design method considering the particularities of UHPFRC should help to better exploit the potential of the material. In general, partial factors of semi-probabilistic design can be calibrated by reliability computations, by experience or estimated by experts’ judgment. The ideal procedure is reliability-based code calibration which ensures the required safety. Such a calibration procedure is for example described by Thoft-Christensen and Baker [6].

In this paper, a calibration of partial factors for the design of non-structural thin UHPFRC elements is presented. The calibration was performed as one of the tasks of C.S.T.B. working group. The calibration itself differs from the original procedure. The original procedure was developed more than 40 years ago and it does not reflect anymore the current computation means and improved knowledge of structural design. The main disadvantage is its inefficient and imprecise iterative loop. The original method also neglects important economic aspects of the code calibration.

## 2. METHODOLOGY OF THE RELIABILITY-BASED CODE CALIBRATIONS

Figure 1 shows an illustrative flow chart of the proposed approach. At the beginning, calibrations points are defined. The calibration points should well approximate the intended domain of applications. The calibration points can be understood as nodes in a mesh describing the multi-dimensional space of the defined scope. Finer the mesh is, better representation of the reality is obtained as in the case of FE simulations. Afterward, two types of computation are performed: a selected design method with various combinations of partial

factors and a probabilistic computation evaluating ratability of each calibration point. At the end, the ideal combination of the partial factors selected. The selection is based on minimizing

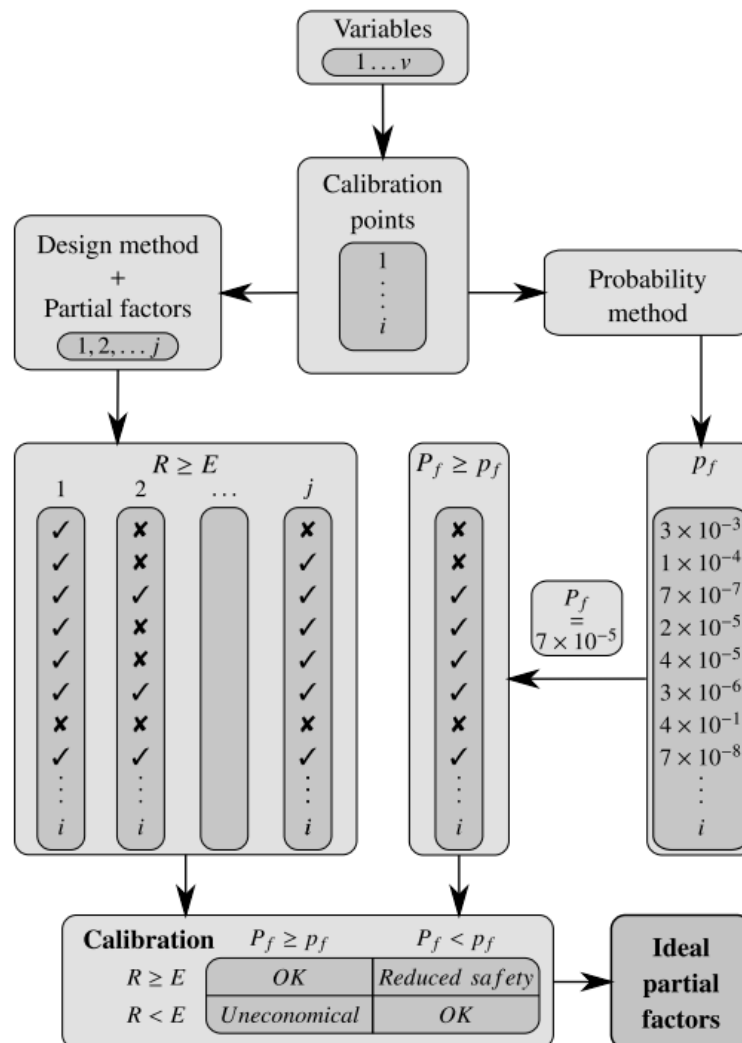


Figure 1: Reliability-based code calibration procedure

The selection is based on minimizing the “non-OK” cells:

$$\min_{\gamma} W(\gamma_j) = \sum_{\text{Reduced safety}} (P^f - p_i^f)^2 w_i + \sum_{\text{Uneconomical}} \alpha (P^f - p_i^f)^2 w_i \quad (1)$$

where  $w$  is the weight of each calibration point and  $\alpha$  is a factor specifying the relative importance of two terms (normally considered as 1). In the extreme case ( $\alpha = 0$ ), a safe optimum would converge to zero situations in the reduced safety cell but at the expense of excessive values in the uneconomical cell. The second term in eq.1 is therefore called a penalty for the excessive safety and it ensures the economic aspects of the code calibration.

Eq. 1 is combined with a scaled conditional probability of occurrence of the situations with the reduced safety in order to limit overpassing the target safety requirements:

$$\tilde{P}_j(P^f < p^f | R \geq E) = \frac{\sum_{R \geq E} w_{i,j}^{scaled}}{\sum_{R \geq E} w_{i,j}^{scaled}} < X_{lim} \quad (2)$$

It is important to mention, that the calibration points in the original procedure are chosen, designed, and optimized to fall into the first row only. However, the calibration points in the new approach are chosen to fully cover the defined scope. Consequently, many points are far from the limit state as they are not optimized but only verified (e.g., thick elements for short spans which would never appear in real applications). Therefore, the weight factor in eq.2 is scaled by  $w_{i,j}^{scaled} = w_i E_{i,j} / R_{i,j}$  to eliminate an influence of the non-realistic calibration points. A use of eqs.1 and 2 guarantees the required safety and at the same time, considers to the economic aspects.

Similarly to the original procedure described by Melchers [7], the new procedure is described with its essential steps.

## 2.1 Define design code format

The design code format was based on EN 1990 [2] thus a semi-probabilistic approach. The design method was developed as an extension of Eurocodes [2, 3, 4, 5] and AFGC 2013 [1] recommendations. All currently used partial factors remained unchanged and only newly introduced factors were calibrated.

## 2.2 Define scope and variables

The design method was developed for thin elements made of UHPFRC which were predominantly loaded in bending without axial forces. The reliability-based code calibration included effects of self-weight, wind, and snow for vertically and horizontally positioned elements.

Table 1: Coordinates of the multi-dimensional mesh / calibration points

Type	Var.	Coordinates	Unit
Material	$f_c$	150	MPa
	$E_{cm}$	40 and 50	GPa
	$f_{ct}$	10, 15 and 20	MPa
	$f_{pc,cc}$	0.6 $f_{ct}$ , 0.8 $f_{ct}$ and 1.0 $f_{ct}$	MPa
	$f_{pc}$	0.6 $f_{ct}$ , 0.8 $f_{ct}$ and 1.0 $f_{ct}$	MPa
	$\epsilon_{pc}$	10 $\epsilon_{el}$ , 20 $\epsilon_{el}$ and 30 $\epsilon_{el}$	(-)
	$\epsilon_{ult}$	0.004 to 0.02	(-)
	$\rho$	2450	kg m <sup>-3</sup>
Dimensions	$L$	600, 1000, 1500, 2000 and 2400	mm
	$h$	20, 40 and 60	mm
	$b$	1000	mm
Loading	$q_s$	0.45, 0.55, 0.65, 0.75, 0.85 and 0.95	kN m <sup>-2</sup>
	$c_s$	0.8, 1.2 and 1.6	(-)
	" $q_w$ "	22, 24, 26 and 28	m s <sup>-1</sup>
	$c_w$	1.0, 2.0, 3.0, 4.0, 5.0, 6.0, 9.0 and 12.0	(-)

The material, dimensions, and loading variables were selected to sufficiently cover the intended domain of applications (Table 1). The precise probability model for the calibration

used all sets of the variables whereas the simple design method used only a simplified constitutive law. Figure 2 shows an uni-axial tensile response, a bending response, and the simplified constitutive law. AFGC 2013 [1] recommendations describe a use of the simplified constitutive law for prediction of the maximal resistance in bending ( $\sigma_{MOR}$ ) and the corresponding deflection ( $d_{MOR}$ ).

### 2.3 Define limit state functions (Design method)

Only one limit state function of an internal failure condition (STR) [2] was relevant for the code calibration. The limit state function was a simplified method adapted from AFGC 2013 [1] recommendations – Annex 4.

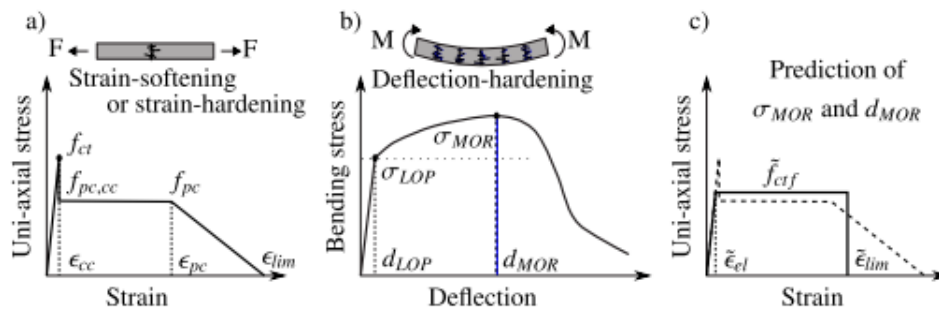


Figure 2: UHPFRC material characteristics: uni-axial tensile response (a), bending response (b), and simplified constitutive law (c)

### 2.4 Define calibration points

The considered materials had deflection-hardening behavior ( $\sigma_{MOR} > \sigma_{LOP}$ ) defined by the compressive strength ( $f_c$ ), the elastic modulus ( $E_{cm}$ ), the elastic bending strength ( $f_{ct}$ ), the immediate post-peak strength ( $f_{pc,cc}$ ), the post-peak strength ( $f_{pc}$ ), the post-peak ductility ( $\epsilon_{pc}$ ), and the ultimate ductility ( $\epsilon_{lim}$ ). The dimensions were defined by the span ( $L$ ), the height ( $h$ ), and the width ( $b$ ). The loading was considered according to French versions of Eurocodes [7, 8, 9, 18, 19] with the snow load ( $q_s$ ), the snow deterministic coefficients ( $c_s$ ), the wind speed (“ $q_w$ ”), and the wind deterministic coefficients ( $c_w$ ). The simplified constitutive law (Figure 1) was defined by the same compressive strength ( $f_c$ ), the same elastic modulus ( $E_{cm}$ ), the simplified elastic bending strength ( $f_{ct,f}$ ), and the simplified ultimate ductility ( $\epsilon_{lim}$ ).

#### 2.4.1 Coordinates

The calibration points were divided into 54 groups based on their material properties ( $1f_c \times 2E_c \times 3f_{ct} \times 3(f_{pc,cc}; f_{pc}) \times 3\epsilon_{pc} \times 1\epsilon_{ult}$ ).  $f_{pc,cc}$  &  $f_{pc}$  represented one calibration point as a post-peak plateau-like response was considered. Strain-hardening or strain-softening behavior was enabled by independent stochastic properties of the immediate post-peak strength ( $f_{pc,cc}$ ) and the post-peak strength ( $f_{pc}$ ). The calibration points were further subdivided into 2 groups based on their orientation. The vertical orientation had 480 possibilities and the horizontal orientation had 3240 possibilities. In total, 200 880 calibration points were defined ( $54 \times (3240 + 480)$ ). Table 2 shows the coordinates of the calibration points.

#### 2.4.2 Weight factor

The individual weights of the coordinates for the given variable were constant for all variables but the wind load. The weights of the wind load were adjusted according to NF EN 1991-1-4: NA [8].

#### 2.4.3 Equivalent calibration points

The design method is based on the simplified constitutive law. During the real design procedure, the inputs for the simplified constitutive law are determined from the experimental tests [1]. In the case of the code calibration, the inputs and their characteristic values had to be determined in an alternative way because there was no direct mathematical relation between the “real” and simplified properties. Therefore, the required experimental tests were simulated by a numerical model [9]. The numerical results were back-analyzed according to AFGC 2013 [1] recommendations so that the sets of values describing the simplified constitutive law ( $f_{ct,f}$ ,  $\epsilon_{lim}$ ) were obtained. The numerical simulation was repeated 1000 times with a Monte Carlo approach for each material group to obtain a sufficient population for determination of the characteristic values. The characteristic values were determined as 5 % lower quantile. The stochastic input parameters for each Monte Carlo repetition are described in Step 10.

#### 2.5 Define partial factors

A partial factor of the simplified bending strength ( $\gamma_f$ ) and a partial factor of the simplified ultimate ductility ( $\gamma_\epsilon$ ) were introduced for the design method described in Step 3. Both factors ranged from 1.0 to 3.5 and were split by 0.1, thus 676 combinations.

#### 2.6. Apply design method

The design method (structural verification) was applied with each combination of the partial factors. The results of the structural verifications were classed into two groups ( $M_{Rd} \geq M_{Ed}$  and  $M_{Rd} < M_{Ed}$ ).

#### 2.7 Define exact method

The exact method is based on a computation of cross-section equilibrium [9].

#### 2.8 Define target reliability

The constant target reliability ( $P_f$ ) for all calibration points was defined according to EN 1990 [2] as  $5 \times 10^{-4}$  for the 50 year reference period and the low consequences class.

#### 2.9 Define reliability method

A reliability method based on a crude Monte Carlo simulation (cMC) was selected to obtain unbiased values of the probability of failure. The cMC simulation allowed using sets of correlated random variables and it did not require any prior knowledge of the simulated problem. 5% relative error for 95% confidence level required at least 3 072 000 repetitions [10]. Nevertheless, 4 000 000 repetitions were chosen for all simulations to cover the medium consequences class [2] ( $P_f = 7 \times 10^{-5}$ , 10% relative error, 90% confidence level,  $\approx 3\,842\,016$ ) if needed later.

#### 2.10 Define partial factors

The partial factors shall account for scatter and uncertainty due to the variables randomness.

### 2.10.1. Distribution functions of random variables

The probability density functions (PDF) of the material and the dimensions were taken from JCSS [11] (when relevant). Log-normal distributions were used for all material properties but the ultimate ductility which had a uniform distribution. The span and thickness had normal distributions. The wind and snow had Gumbel Type-I distributions. The mean values of each variable were the coordinates shown in Table 2. The elastic material properties had coefficients of variation (CoV) of 0.1 and the nonlinear material properties had CoVs of 0.2 due to higher uncertainty. The immediate post-peak strength ( $f_{pc,cc}$ ) had a variable CoV; 0.10 when there was no drop at the onset of cracking, 0.15 when there was a drop of 20 % ( $0.8 f_{ct}$ ) and 0.20 when there was a drop of 40% ( $0.6 f_{ct}$ ). The dimensions had the same nominal standard deviations (10mm and 0.5mm) as the same quality control was assumed for all spans and for all thicknesses, respectively. The CoV of wind was 0.2 and 0.3 for snow. The experimental samples (Step 4) had the span 420mm, the width 150mm, and the thickness 40mm. The span and the thickness were considered as stochastic properties with the same standard deviations of 1mm.

### 2.10.2. Samples of random variables

The cMC simulation (Step 9) used 4 000 000 samples for each variable. The samples were independently drawn from the cumulative distribution functions by generating uniform random values (0, 1). The exact procedure can be found elsewhere [10, 12].

### 2.10.3. Statistical correlation of random variables

The samples of the random variables were generated without any requirement on their statistical correlation. In reality, some variables are correlated ( $\rho \neq 0$ ) and others are uncorrelated ( $\rho = 0$ ). Table 2 shows a part of a correlation matrix used for the code calibration. All unmentioned values were assumed to be zero (i.e., uncorrelated) due to natural randomness or due to a lack of data providing correlations. In addition to the correlation matrix, the random variables were further constrained by physical conditions of the material law:  $f_{ct} \geq f_{pc,cc}$  and  $\epsilon_{pc} < \epsilon_{ult}$

Table 2: Correlation matrix of random variables

	$f_c$	$E_c$	$f_{ct}$	$f_{pc,cc}$	$f_{pc}$	$\epsilon_{pc}$	$\epsilon_{lim}$
$f_c$	1	0.6	0.6				
$E_c$	0.6	1	0.6				
$f_{ct}$	0.6	0.6	1	(0.4 – 1.0)			
$f_{pc,cc}$			(0.4 – 1.0)	1	0.1		
$f_{pc}$				0.1	1	-0.2	
$\epsilon_{pc}$					-0.2	1	$\frac{2\epsilon_{pc}}{3\epsilon_{lim}}$
$\epsilon_{ult}$						$\frac{2\epsilon_{pc}}{3\epsilon_{lim}}$	1

### 2.10.4. Method to obtain targeted statistical correlation of random variables

The desired correlation coefficients were obtained by rearranging the samples. Such a procedure did not influence the PDFs of the selected samples and allowed to prescribe the additional constraints [12, 13]

### 2.11 Apply reliability method

The calibration points were grouped by material properties (54 types of material) and each group was simulated independently. Each simulation consisted of two parts: a computation of the cross-section resistance and a computation of the applied load. The computations were repeated for all sets of the correlated random variables ( $t=4.000.000$ ). It is worth mentioning that the resistance and the applied loads were positively correlated due to the thickness of the elements. The computation of the resistance was made for each thickness ( $R_i^t$ ,  $i=3$ ). The computation of the applied load was made for all permissible combinations of the input variables ( $R_{i,j}^t$ ,  $j=3720$ ). The probability of failure of each combination was then computed as:

$$p_f^{i,j} = \frac{1}{n} \sum_{t=1}^n X_{i,j}^t \quad (3)$$

where  $X_{i,j}^t$  was a failure counter influenced by the model uncertainty ( $U_j^t$ ) The failure counter was defined as:

$$X_{i,j}^t = 1 \quad \text{if} \quad R_i^t U_j^t < E_{i,j}^t \quad \text{and} \quad X_{i,j}^t = 0 \quad \text{otherwise} \quad (4)$$

JCSS [14] defines various functions for the model uncertainty which depend on loading and resistance characteristics. It was assumed that there was no uncertainty related to the load effects on simply supported beams. The exact method defined in Step 7 was based on the clear and scientifically well-founded theories and therefore its uncertainty was low. Thus, a log-normal distribution ( $\mu=1.0$ ,  $CoV=0.05$ ) was assumed for the uncertainty of the resistance model [11]. Zero correlations factors were considered for all variables as well as for other model uncertainties (Table 2).

### 2.12 Select partial factors

The ideal partial factors were selected by the optimization procedure based on eqs.1 and 2 considering the following assumptions:

- (i) Low consequence reliability class ( $\beta = 3.3$ ;  $p_f = 5 \times 10^{-4}$ , [2]);
- (ii) Same relative importance of uneconomical situations and situations with the reduced safety; i.e.,  $\alpha = 1$  in eq.1;
- (iii) Horizontal and vertical panels with the same probability of occurrence;  $X_{lim}=0.05$ , eq.2

## 3. RESULTS

The reliability-based code calibration was performed considering the selection criterion from Step 12: the minimization criteria eq.1 and the scaled conditional probability of occurrence of the situations with the reduced safety eq.2. Figure 3 shows the outputs from the reliability-based code calibration procedure.

### 3.1. Ideal partial factors

In Figure 3, the partial factors of  $\gamma_\varepsilon = 2.0$  and  $\gamma_f = 2.5$  are marked. These factors fulfilled the limiting conditions defined in Step 12.

### 3.2. Structural verification

Figure 4 shows two loading histograms for a brittle-like (left) and a ductile-like (right) material where  $f_{LOP}$  is the Limit of Proportionality and  $f_{MOR}$  is the Modulus of Rapture. The

new semi-probabilistic design clearly differentiates between brittle-like and ductile-like behavior. The resistance of the brittle material is similar to the original brittle-design method whereas the design resistance of the “ductile” material is significantly increased due to the substantial contribution of the fibers.

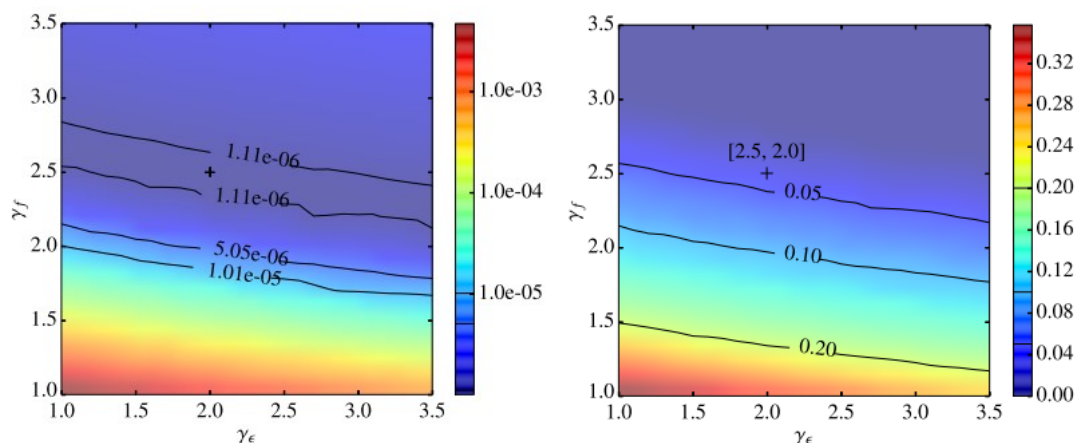


Figure 3: Development of the minimization criteria eq.1 (a) and Development of the scaled conditional probability of occurrence of situations with the reduced safety eq.2; Three contours are highlighted for better clarity.

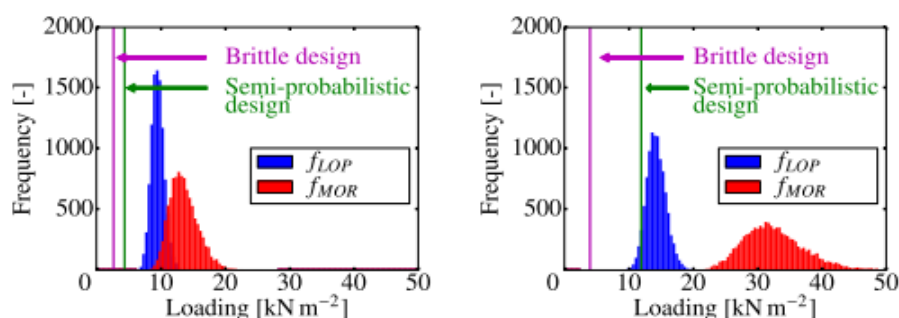


Figure 4: Histograms of loading leading to cracking ( $f_{LOP}$ ) and to the maximal resistance ( $f_{MOR}$ ) for a brittle-like (left) and a ductile-like (right) material together with the design resistances of the original brittle design approach and the new semi-probabilistic approach

#### 4. CONCLUSIONS

The semi-probabilistic approach used in the current design codes requires calibrated partial factors to secure the safety of structures and people. The original code calibration procedure does not reflect the recent development of computation tools and improved knowledge of structural design. The main disadvantage is its inefficient and imprecise iterative loop during the calibration. Moreover, the original procedure neglects economic aspects which should be an integral part of any code calibration.

The new approach was used to calibrate the partial factors for the structural verification of UHPRC thin elements predominantly loaded in bending. At the beginning, the scope and relevant variables were defined. The variables were defined both deterministically and stochastically. The stochastic properties included the statistical correlation of all random variables. The code calibration computation covered more than 200 000 calibration points.

The crude Monte Carlo simulation was used for the reliability computation. 4 000 000 simulations for each calibration point ensured the small relative error (below 5%) with the 95 % confidence level.

The ideal partial factors for ductility and strength are equal to 2.0 and 2.5, respectively. The values were calibrated for the low consequence reliability class ( $\beta = 3.3$ ;  $p_f = 5 \times 10^{-4}$ ), including both horizontally and vertically oriented elements.

The results provide compelling evidence of the advantages of the reliability-based code calibration and notably the advantages of the new approach. Indeed, the design method of non-structural UHPFRC thin elements with the calibrated partial factors allows better exploitation of the material without compromising the safety requirements. The complete structural verification of thin elements made of UHPFRC is based on Ultimate Limit State design using the defined partial factors as well as on Service Limit State design which can be a governing scenario in some cases.

It is worth noting that the calibrated partial factors can be used for the defined scope only.

## ACKNOWLEDGEMENTS

The authors would like to thank the C.S.T.B working group for providing and/or confirming the inputs for the code calibration

## REFERENCES

- [1] AFGC 2013, Ultra high performance fibre-reinforced concretes - Recommendations. AFGC working group on UHPFRC, co-ordinated by Jocelyne Jacob and Pierre Marchand.
- [2] NF EN 1990 Eurocode: Basis of structural design. AFNOR French standard institute.
- [3] NF EN 1991-1-1 Eurocode 1: Actions on structures - Part 1-1: General actions Densities, self-weight, imposed loads for buildings. AFNOR French standard institute.
- [4] NF EN 1991-1-3 Eurocode 1: Actions on structures - Part 1-3: General actions Snow loads. AFNOR French standard institute.
- [5] NF EN 1991-1-4 Eurocode 1: Actions on structures - Part 1-4: General actions Wind actions. AFNOR French standard institute.
- [6] Thoft-Christensen, P., Baker, M., 1982. Structural reliability theory and its applications. Springer-Verlag.
- [7] Melchers, R., 1999. Structural Reliability Analysis and Prediction, second edition Edition. John Wiley & Sons Ltd.
- [8] NF EN 1991-1-4 Eurocode 1: Actions sur les structures - Part 1-4: Actions generales Actions du vent – Annexe nationale a la NF EN 1991-1-4:2005. AFNOR French standard institute.
- [9] Dobrusky, S., Chanvillard, G., 2014. Modified force-based fiber beam formulation tailored for inverse analysis of both strain hardening and strain softening cementitious composites. In: PRO 97: 3rd International RILEM Conference on Strain Hardening Cementitious Composites (SHCC3-Delft). RILEM Publication S.A.R.L., pp. 219–226.
- [10] Rao, S. S., 1992. Reliability-based design. McGraw-Hill, Inc.
- [11] JCSS, 2001. Probabilistic Model Code. JCSS-OSTL / DIA / VROU-10-11-2000. Joint Committee on Structural Safety, 12<sup>th</sup> draft.
- [12] Vorechovsky, M., 2004. Stochastic fracture mechanics and size effect. Ph.D. thesis, Brno University of Technology, Czech Republic.
- [13] Iman, R. L., Conover, W., 1982. A distribution-free approach to inducing rank correlation among input variables. Communications in Statistics Simulation and Computation 11 (3), 311–334.